THE STRUCTURE OF THE NEAR-TIP FIELD DURING TRANSIENT ELASTODYNAMIC CRACK GROWTH

L. B. FREUND

Division of Engineering, Brown University, Providence, RI 02912, U.S.A.

and

A. J. ROSAKIS

Graduate Aeronautical Laboratories, California Institute of Technology,
Pasadena, CA 91125, U.S.A.

ABSTRACT

THE PROCESS of dynamic crack growth in a nominally elastic material under conditions of plane strain or plane stress is considered. Of particular concern is the influence of the transient nature of the process on the stress field in the immediate vicinity of the crack tip during nonsteady growth. Asymptotically, the crack tip stress field is square root singular at the crack tip, with the angular variation of the singular field depending weakly on the instantaneous crack tip speed and with the instantaneous stress intensity factor being a scalar multiplier of the singular field. However, for a material particle at a small distance from the moving crack, the local stress field depends not only on instantaneous values of crack speed and stress intensity factor, but also on the past history of these time-dependent quantities. A representation of the crack tip field is obtained in the form of an expansion about the crack tip in powers of radial coordinate, with the coefficients depending on the time rates of change of crack tip speed and stress intensity factor. This representation is used to interpret some experimental observations, with the conclusion that the higher-order expansion provides an accurate description of crack tip fields under fairly severe transient conditions. In addition, some estimates are made of the practical limits of using a stress intensity factor field alone to characterize the local fields.

INTRODUCTION

ONE OF the cornerstone concepts of linear elastic fracture mechanics is the role of the stress intensity factor as a crack tip field characterizing parameter. IRWIN (1957) observed that the elastic stress field near the tip of a crack which opens symmetrically (mode I opening) has the now familiar form

$$\sigma_{ij} = \frac{K_I}{\sqrt{2\pi r}} \Sigma_{ij}(\theta) + O(1) \quad \text{as} \quad r \to 0$$

in a polar coordinate system centered at the crack tip. The dependence on radial coordinate r is explicit, and the angular variation functions Σ_{ij} can be expressed in terms of trigonometric functions of angle θ. The leading term in an asymptotic

expansion of the crack tip field in powers of r is thus universal. The only feature which varies with loading conditions and geometrical configuration of the cracked body is the scalar multiplier, the elastic stress intensity factor K_I. For strictly two-dimensional deformations, the above field can be valid only within a region near the crack tip which is small compared to the crack length, distance to the nearest boundary, or any other characteristic dimension of the body. On the other hand, the assumption of a two-dimensional elastic field cannot be valid right up to the crack tip, even under plane strain conditions. Within some small region near the tip, the two-dimensional elastic field must give way to a region of inelastic deformation. Nonetheless, if this inelastic zone is completely surrounded by a stress intensity factor field, then it is commonly assumed that the stress intensity factor can be used to characterize the fracture process and that fracture will begin when the value of stress intensity factor has been increased to a material-specific value, the fracture toughness of the material.

When the stress intensity factor idea is applied to the case of a through-the-thickness crack in a plate, the restrictions become somewhat more severe if the process is to be characterized in terms of a stress intensity factor associated with a two-dimensional state of plane stress. In addition to the limitation noted above concerning overall body dimensions and crack length, such points must also be far enough from the crack edge to be *outside* the zone of influence of three-dimensional effects around the crack edge. Typically, the plane stress assumption is valid only for $r > h/2$, where h is the plate thickness (ROSAKIS and RAVI-CHANDAR, 1986; YANG and FREUND, 1986).

If the crack growth process in a plate is dynamic, so that the inertia of the material comes into play, there is yet another factor which complicates the application of the stress intensity factor idea under conditions of plane stress. This factor is due to the wave character of the mechanical fields in the body during crack growth. To illustrate this effect, consider a crack growing dynamically at a constant speed. Suppose that, at equally spaced intervals of time, wave signals are emitted from the crack tip. A set of such waves is illustrated schematically in Fig. 1, where the circles represent wavefronts of the signals. The centers of the circles are located at equally spaced points along the crack growth direction. Consider a particular field point P that is near to the crack tip in some sense. It is then clear from the diagram that this point is far behind the wavefronts emitted earliest, compared to the distance from P to the crack
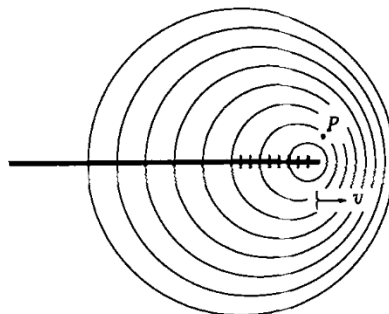

FIG. 1. Schematic diagram illustrating the potentially complex dependence of the stress field at a point near the crack tip on the recent past history of crack speed and stress intensity factor during transient crack growth.

tip. On the other hand, the point is outside of the wavefronts emitted most recently. If information measured at this point, as well as at similar points around the crack edge, is used to infer something about the value of the stress intensity factor, then the wave nature of the fields should be considered. In some sense, local measurements sense the recent *history* of the stress intensity factor. If the stress intensity factor is essentially constant during this time, then the effect is obviously negligible. However, if the stress intensity factor is varying rapidly in time, then its value may change significantly during the time of influence at P and the existence of a region of practically significant size around the crack edge in which the field is characterized by the instantaneous value of stress intensity factor is uncertain. The possibility that the extent of the stress intensity factor during dynamic crack growth under transient conditions is more limited than a steady-state analysis would indicate was first suggested by the analysis of MA and FREUND (1986).

The purpose of the present study is two-fold. First, a higher-order asymptotic expansion of crack tip fields under plane stress conditions is obtained for transient crack growth. In the present context, transient crack growth is understood to include processes in which both the crack tip speed and the dynamic stress intensity factor are differentiable functions of time. The analytical result is used to interpret some experimental observations, with the conclusion that the higher-order expansion provides a good representation of crack tip fields under fairly severe transient conditions. Then, some estimates are made of the practical limits of using a stress intensity factor field alone to characterize the local fields.

GOVERNING EQUATIONS FOR PLANE STRESS ELASTODYNAMIC CRACK GROWTH

Consider a homogeneous and isotropic linear elastic solid occupying a two-dimensional region in the x'_1, x'_2-plane. The outer boundary is subjected to traction and/or displacement boundary conditions of a type to ensure uniqueness of solutions. Suppose that a planar crack grows through the body with nonuniform crack speed $v(t)$. Within the framework of the theory of plane stress, the two-dimensional displacement vector **u** is governed by the equation (FREUND, 1990)

$$c_l^2 \nabla(\nabla \cdot \mathbf{u}) - c_s^2 \nabla \wedge \nabla \wedge \mathbf{u} = \ddot{\mathbf{u}}, \tag{1}$$

where ∇ is the two-dimensional gradient operator and a superposed dot indicates differentiation with respect to time. In terms of Young's modulus E and Poisson's ratio v, the longitudinal and shear wave speeds for plane stress are

$$c_l = [E/(1-v^2)\rho]^{1/2} \quad \text{and} \quad c_s = [E/2(1+v)\rho]^{1/2},$$

respectively, where ρ is the material mass density.

Any displacement **u** which is derived from longitudinal and shear wave potentials $\phi(x'_1, x'_2, t)$ and $\psi(x'_1, x'_2, t)$ according to

$$\mathbf{u} = \nabla\phi + \nabla \wedge \psi \tag{2}$$

with

$$c_l^2 \nabla^2 \phi - \ddot{\phi} = 0, \quad c_s^2 \nabla^2 \psi - \ddot{\psi} = 0 \qquad (3)$$

satisfies (1). Conversely, any solution of (1) has the representation (2). In plane stress ψ has a single nonzero component denoted here by ψ.

Suppose that a translating coordinate system (x_1, x_2) is introduced with its origin at the moving crack tip and oriented with the x_1-axis aligned with the direction of crack growth. The displacement potentials can then be viewed as functions of position in the moving coordinate system, as well as time. The new functions are denoted by Φ and Ψ, that is, $\Phi(x_1, x_2, t) = \phi(x'_1, x'_2, t)$ and $\Psi(x_1, x_2, t) = \psi(x'_1, x'_2, t)$. Under the transformation of coordinates, the partial differential equation (3) governing the longitudinal displacement potential becomes

$$\frac{\partial^2 \Phi}{\partial x_1^2}\left(1 - \frac{v^2}{c_l^2}\right) + \frac{\partial \Phi}{\partial x_2^2} + \frac{\dot{v}}{c_l^2}\frac{\partial \Phi}{\partial x_1} + 2\frac{v}{c_l^2}\frac{\partial^2 \Phi}{\partial x_1 \partial t} - \frac{1}{c_l^2}\frac{\partial \Phi}{\partial t^2} = 0. \qquad (4)$$

The shear wave potential $\Psi(x_1, x_2, t)$ satisfies the same equation with c_l replaced by c_s. It is also noted for future reference that the first scalar invariant of stress for the assumed state of plane stress is determined by the displacement potential Φ according to

$$\sigma_{11} + \sigma_{22} = 2\rho(c_l^2 - c_s^2)\nabla_x^2 \Phi, \qquad (5)$$

where ∇_x^2 is the Laplacian operator in the translating coordinate system.

Asymptotic Crack Tip Field for Transient Crack Growth

To derive an asymptotic expansion for the stress components as $r = \sqrt{x_1^2 + x_2^2} \to 0$, a standard device is employed whereby the region around the crack tip is expanded so it fills the entire field of observation (Freund, 1990). To this end, rescaled coordinates $\eta_\alpha = x_\alpha/\varepsilon$ are introduced, with $\varepsilon > 0$ being a small parameter and $\alpha = 1$ or 2. As $\varepsilon \to 0$, all points in the x_1, x_2-plane except those near the crack tip are mapped beyond the range of observation in the η_1, η_2-plane.

It is assumed that Φ has an expansion in powers of ε of the form

$$\Phi(x_1, x_2, t) = \Phi(\varepsilon\eta_1, \varepsilon\eta_2, t) = \sum_{m=0}^{\infty} \varepsilon^{(m+3)/2}\Phi_m(\eta_1, \eta_2, t), \qquad (6)$$

where Φ_0 represents the main contribution to the asymptotic solution, Φ_1 represents the first-order correction, and so on. The first term of this series ($m = 0$) corresponds to the expected square root singular contribution proportional to $r^{-1/2}$ in the asymptotic near-tip stress field.

The assumed asymptotic form (6) is substituted into the governing equation (4) and the coefficient of each power of ε is set equal to zero to obtain a system of coupled differential equations for Φ_m. The first several such equations are

$$\alpha_l^2 \frac{\partial^2 \Phi_0}{\partial \eta_1^2} + \frac{\partial^2 \Phi_0}{\partial \eta_2^2} = 0, \tag{7a}$$

$$\alpha_l^2 \frac{\partial^2 \Phi_1}{\partial \eta_1^2} + \frac{\partial^2 \Phi_1}{\partial \eta_2^2} = 0, \tag{7b}$$

$$\alpha_l^2 \frac{\partial^2 \Phi_2}{\partial \eta_1^2} + \frac{\partial^2 \Phi_2}{\partial \eta_2^2} = -\frac{2v^{1/2}}{c_l^2} \frac{\partial}{\partial t} \left\{ v^{1/2} \frac{\partial \Phi_0}{\partial \eta_1} \right\}, \tag{7c}$$

$$\alpha_l^2 \frac{\partial^2 \Phi_3}{\partial \eta_1^2} + \frac{\partial^2 \Phi_3}{\partial \eta_2^2} = -\frac{2v^{1/2}}{c_l^2} \frac{\partial}{\partial t} \left\{ v^{1/2} \frac{\partial \Phi_1}{\partial \eta_1} \right\}, \tag{7d}$$

$$\alpha_l^2 \frac{\partial^2 \Phi_4}{\partial \eta_1^2} + \frac{\partial^2 \Phi_4}{\partial \eta_2^2} = -\frac{2v^{1/2}}{c_l^2} \frac{\partial}{\partial t} \left\{ v^{1/2} \frac{\partial \Phi_2}{\partial \eta_1} \right\} + \frac{1}{c_l^2} \frac{\partial^2 \Phi_0}{\partial t^2}, \tag{7e}$$

$$\alpha_l^2 \frac{\partial^2 \Phi_5}{\partial \eta_1^2} + \frac{\partial^2 \Phi_5}{\partial \eta_2^2} = -\frac{2v^{1/2}}{c_l^2} \frac{\partial}{\partial t} \left\{ v^{1/2} \frac{\partial \Phi_3}{\partial \eta_1} \right\} + \frac{1}{c_l^2} \frac{\partial^2 \Phi_1}{\partial t^2}, \tag{7f}$$

and so on, where $\alpha_l = (1 - v^2/c_l^2)^{1/2}$.

For any value of m, the governing equation has the general form

$$\alpha_l^2 \frac{\partial^2 \Phi_m}{\partial \eta_1^2} + \frac{\partial^2 \Phi_m}{\partial \eta_2^2} = -\frac{2v^{1/2}}{c_l^2} \frac{\partial}{\partial t} \left\{ v^{1/2} \frac{\partial \Phi_{m-2}}{\partial \eta_1} \right\} + \frac{1}{c_l^2} \frac{\partial^2 \Phi_{m-4}}{\partial t^2}, \tag{8}$$

for $m = 0, 1, 2, \ldots$, where $\Phi_k \equiv 0$ if $k < 0$. The shear wave potential Ψ is also assumed to be expressible in terms of a similar expansion for ε, with coefficients Ψ_m satisfying an equation similar to (8) with c_l replaced by c_s.

It is noted that, for the special case of *steady-state* crack growth, $\dot{v} = 0$ and $\partial \Phi_m / \partial t = 0$ for $m = 0, 1, 2, \ldots$ In such a case, the equations (7) are not coupled and each reduces to Laplace's equation in the coordinates η_1, $\alpha_l \eta_2$. The solution for this case is discussed by DALLY (1987) who attributes the original results to unpublished work of G. R. Irwin. The corresponding functions Φ_m are independent of time in the moving coordinate system. In the general transient case, on the other hand, the only uncoupled equations are those for $m = 0$ and $m = 1$. Indeed, as will be seen, Φ_0 and Φ_1 have the same spatial structure in both the transient and the steady-state cases. This is not so, however, for Φ_m if $m > 1$.

An expansion for the first stress invariant in the scaled coordinate system (η_1, η_2) can be obtained from (5) and (6) as

$$\sigma_{11} + \sigma_{22} = 2\rho(c_l^2 - c_s^2) \sum_{m=0}^{\infty} \varepsilon^{(m-1)/2} \left[\frac{\partial \Phi_m}{\partial \eta_1^2} + \frac{\partial \Phi_m}{\partial \eta_2^2} \right]. \tag{9}$$

In view of (8), this expression can be rewritten as

$$\frac{\sigma_{11} + \sigma_{22}}{2\rho(c_l^2 - c_s^2)} = \sum_{m=0}^{\infty} \varepsilon^{(m-1)/2} \left[\frac{v^2}{c_l^2} \frac{\partial^2 \Phi_m}{\partial \eta_1^2} - \frac{2v^{1/2}}{c_l^2} \frac{\partial}{\partial t} \left\{ v^{1/2} \frac{\partial \Phi_{m-2}}{\partial \eta_1} \right\} + \frac{1}{c_l^2} \frac{\partial^2 \Phi_{m-4}}{\partial t^2} \right]. \tag{10}$$

This relation does not involve derivatives of Φ_m with respect to η_2.

The Case of Transient Crack Growth at Constant Velocity

In this section, a special case of transient crack growth is considered, namely, crack propagation with constant crack tip speed v but with a time-dependent stress intensity factor. Although the crack tip speed is constant in this case, the potential functions Φ and Ψ are still time-dependent, in general, and the right side of (8) is not identically zero as it is in steady-state crack growth. Crack growth phenomena having this behavior have been observed by RAVI-CHANDAR and KNAUSS (1987) and ·ROSAKIS *et al.* (1984), among others. A mathematical model having this feature is provided by the plane stress problem of a crack suddenly beginning to grow symmetrically at constant rate from zero initial length in a uniform body subjected to a remote tensile field. The solution of this problem was first obtained by BROBERG (1960). As is evident from the analytic solution of the Broberg problem, which is considered in detail in FREUND (1990), the stress intensity factor is a function of time. In fact, based on dimensional considerations, the stress intensity factor varies in proportion to time t raised to the power one-half. The Broberg solution will be examined further in a subsequent section.

The equations (7) may be solved sequentially, and the first steps for $m = 0$ and $m = 1$ have been presented by FREUND (1990). For these cases, the solutions for symmetric modes of crack growth are

$$\hat{\Phi}_m(r_l, \theta_l, t) = A_m(t)r_l^{(m+3)/2} \cos \tfrac{1}{2}(m+3)\theta_l, \quad m = 0, 1 \tag{11}$$

where $r_l^2 = (\eta_1^2 + \alpha_l^2 \eta_2^2)$ and $\theta_l = \tan^{-1}(\alpha_l \eta_2/\eta_1)$. Note that $\hat{\Phi}_m(r_l, \theta_l, t) = \varepsilon^{(m+3)/2}\Phi_m(\eta_1, \eta_2, t)$ by definition. For constant velocity crack growth, (r_l, θ_l) are translating polar coordinates distorted from conventional polar coordinates by an amount determined by the crack speed v. Because v is constant, the coordinates (r_l, θ_l) are time-independent. Time enters the solution (11) only through the coefficients $A_m(t)$. By definition, the coefficient $A_0(t)$ is related to the stress intensity factor (FREUND, 1990) by

$$A_0(t) = -\frac{4K_I^d(t)}{2\mu\sqrt{2\pi}} \frac{1+\alpha_s^2}{\Delta(v)},$$

where $K_I^d(t)$ is the time-dependent dynamic stress intensity factor and $\Delta(v) = 4\alpha_l\alpha_s - (1+\alpha_s^2)^2$.

The functions $\hat{\Phi}_2$ and $\hat{\Phi}_3$ are obtained by solving (8) for $m = 2$ and 3. For these values of m, (8) reduces to

$$\alpha_l^2 \frac{\partial^2 \Phi_m}{\partial \eta_1^2} + \frac{\partial \Phi_m}{\partial \eta_2^2} = -\frac{2v}{c_l^2} \frac{\partial^2 \Phi_{m-2}}{\partial t \, \partial \eta_1}. \tag{12}$$

The result of substituting (11) into the right side of (12) and converting to the distorted polar coordinates (r_l, θ_l) is

$$\nabla_l^2 \hat{\Phi}_m \equiv \frac{\partial^2 \hat{\Phi}_m}{\partial r_l^2} + \frac{1}{r_l} \frac{\partial \hat{\Phi}_m}{\partial r_l} + \frac{1}{r_l^2} \frac{\partial^2 \hat{\Phi}_m}{\partial \theta_l^2} = D^{-1}[A_{m-2}]r_l^{(m-1)/2} \cos \tfrac{1}{2}(m-1)\theta_l, \tag{13}$$

where $D^{-1}[A_k]$ denotes the operator

$$D^1[A_k] = -\frac{(k+3)v^{1/2}}{\alpha_l^2 c_l^2}\frac{\mathrm{d}}{\mathrm{d}t}\{v^{1/2}A_k\}$$

for $k = 0, 1, 2, 3, \ldots$, which reduces to

$$D^1[A_k] = -\frac{(k+3)v}{\alpha_l^2 c_l^2}\frac{\mathrm{d}A_k}{\mathrm{d}t}$$

for constant-velocity crack growth. In the development to follow, this operator is understood to yield $D^1[A_k] \equiv 0$ for $k < 0$.

Relation (13) holds only for $m = 0, 1, 2$ or 3. The general solution for these values of m and symmetric mode I crack growth is

$$\hat{\Phi}_m = r_l^{(m+3)/2}\left\{A_m(t)\cos\tfrac{1}{2}(m+3)\theta_l + \frac{D^1[A_{m-2}(t)]}{2m+2}\cos\tfrac{1}{2}(m-1)\theta_l\right\}, \qquad (14)$$

which also applies only for $m = 0, 1, 2$ or 3. Note that (11) is a special case of (14) which corresponds to $m = 0$ or 1. For $m = 4$ or 5 the procedure is continued, in which case (8) becomes

$$\alpha_l^2\frac{\partial^2\Phi_m}{\partial\eta_1^2} + \frac{\partial\Phi_m}{\partial\eta_2^2} = -\frac{2v}{c_l^2}\frac{\partial^2\Phi_{m-2}}{\partial t\,\partial\eta_1} + \frac{1}{c_l^2}\frac{\partial^2\Phi_{m-4}}{\partial t^2}. \qquad (15)$$

If the potential Φ_m is again viewed as a function of the scaled polar coordinates (r_l, θ_l), and if (14) is substituted into the right side of (15), then $\hat{\Phi}(r_l, \theta_l, t)$ must satisfy the partial differential equation

$$\nabla_l^2\hat{\Phi}_m(r_l, \theta_l, t) = \left\{\left[D^1[A_{m-2}(t)] + \frac{D^2[A_{m-4}(t)]}{(m-1)^2} + \ddot{A}_{m-4}\right]\cos\tfrac{1}{2}(m-1)\theta_l\right.$$

$$\left. + \frac{D^2[A_{m-4}(t)]}{2(m-1)}\cos\tfrac{1}{2}(m-5)\theta_l\right\}r_l^{(m-1)/2}, \qquad (16)$$

where

$$D^2[A_k] = D^1[D^1[A_k]], \quad \ddot{A}_k = \frac{1}{\alpha_l^2 c_l^2}\frac{\mathrm{d}^2 A_k}{\mathrm{d}t^2}$$

for $k = 0, 1, \ldots$ Note that (16) holds only for integers $m = 1, \ldots, 5$. The general solution of (16) for mode I crack growth is

$$\hat{\Phi}_m(r_l, \theta_l, t) = r^{(m+3)/2}\left\{A_m(t)\cos\tfrac{1}{2}(m+3)\theta_l\right.$$

$$+ \frac{1}{2(m+1)}\left[D^1[A_{m-2}(t)] + \frac{D^2[A_{m-4}(t)]}{(m-1)^2} + \ddot{A}_{m-4}\right]\cos\tfrac{1}{2}(m-1)\theta_l$$

$$\left. + \frac{D^2[A_{m-4}(t)]}{8(m-1)^2}\cos\tfrac{1}{2}(m-2)\theta_l\right\} \qquad (17)$$

for $m = 1, \ldots, 5$. It is clear that (11) and (14) are special cases of (17) for $m = 0$ or 1 and $m = 0, 1, 2$ or 3, respectively.

A six-term expansion for the stress invariant as a function of position around the crack tip can be obtained by substituting (17) into (10). If the terms in the series are written out explicitly, then this expansion is

$$
\frac{\sigma_{11}+\sigma_{22}}{2\rho(c_l^2-c_s^2)} = \frac{3\dot{a}^2}{4c_l^2} A_0 r_l^{-1/2} \cos \tfrac{1}{2}\theta_l + \frac{2\dot{a}^2}{c_l^2} A_1
$$

$$
+ \left\{ \left[\frac{15\dot{a}^2}{4c_l^2} A_2 + \left(1 - \frac{\dot{a}^2}{2c_l^2}\right) D^1[A_0] \right] \cos \tfrac{1}{2}\theta_l + \frac{\dot{a}^2}{8c_l^2} D^1[A_0] \cos \tfrac{3}{2}\theta_l \right\} r_l^{1/2}
$$

$$
+ \left\{ \left[\frac{6\dot{a}^2}{c_l^2} A_3 + \left(1 - \frac{\dot{a}^2}{4c_l^2}\right) D^1[A_1] \right] \cos \theta_l \right\} r_l
$$

$$
+ \left\{ \left[\frac{35\dot{a}^2}{4c_l^2} A_4 + \left(1 - \frac{\dot{a}^2}{2c_l^2}\right) D^1[A_2] + \frac{1}{9}\left(1 - \frac{\dot{a}^2}{4c_l^2}\right) D^2[A_0] + \left(1 - \frac{\dot{a}^2}{2c_l^2}\right) \ddot{A}_0 \right] \cos \tfrac{3}{2}\theta_l \right.
$$

$$
+ \left[\frac{3\dot{a}^2}{8c_l^2} D^1[A_2] + \frac{1}{6}\left(1 - \frac{\dot{a}^2}{4c_l^2}\right) D^2[A_0] + \frac{3\dot{a}^2}{8c_l^2} \ddot{A}_0 \right] \cos \tfrac{1}{2}\theta_l + \frac{\dot{a}^2}{96c_l^2} D^2[A_0] \cos \tfrac{5}{2}\theta_l \left. \right\} r_l^{3/2}
$$

$$
+ \left\{ \left[\frac{12\dot{a}^2}{c_l^2} A_5 + \left(1 - \frac{\dot{a}^2}{2c_l^2}\right) D^1[A_3] + \frac{1}{16} D^2[A_1] + \left(1 - \frac{\dot{a}^2}{2c_l^2}\right) \ddot{A}_1 \right] \cos 2\theta_l \right.
$$

$$
+ \left[\frac{\dot{a}^2}{2c_l^2} D^1[A_3] + \frac{1}{8}\left(1 - \frac{\dot{a}^2}{4c_l^2}\right) D^2[A_1] + \frac{\dot{a}^2}{2c_l^2} \ddot{A}_1 \right] \left. \right\} r_l^2 + o(r_l^2), \tag{18}
$$

where $D^1[A_k]$ was introduced in (13) and $D^2[A_k]$ was introduced in (16). Note that the spatial variation of the terms in this expansion with coefficients A_k are identical to those obtained from an asymptotic analysis under the assumption of steady-state crack growth. Of course, in the general transient case, the quantities represented by A_k are functions of time. Also, $D^1[A_k]$, $D^2[A_k]$ and $\ddot{A}_k$ are normalized derivatives with respect to time of the coefficients A_k. For example, for constant velocity v but time-dependent stress intensity factor $K_I^d(t)$, the quantity $D^1[A_0]$ can be reduced to the first time derivative of the stress intensity factor,

$$
D^1[A_0] = \frac{4v(1+\alpha_s^2)}{\mu \alpha_l^2 c_l^2 \sqrt{2\pi\Delta(v)}} \frac{\mathrm{d}K_I^d}{\mathrm{d}t} \tag{19}
$$

COMPARISON WITH CONSTANT-VELOCITY EXPERIMENTS

In this section, some experimental results on rapid crack propagation are interpreted on the basis of the foregoing asymptotic analysis. The main purpose is to determine if the crack tip fields actually observed in the vicinity of dynamically growing fractures can be represented by the fields anticipated in the higher-order asymptotic analysis.

The comparison is restricted to the case in which transient crack growth is indeed observed to occur with constant crack speed, following fracture initiation.

A full-field optical technique, called the coherent gradient sensing (CGS) method, has been developed by TIPPUR *et al.* (1989) for measuring crack tip deformation fields. This method can be used in either transmission mode for transparent materials or in reflection mode for opaque materials. Like the well-known method of caustics, the CGS method is based on the detection of gradients in the optical path caused by deformation of a nominally two-dimensional sample. In transmission mode, these gradients arise from changes in refractive index of the material due to nonuniform strain in the sample, while in reflection mode they arise from changes in slope of the sample surface due to nonuniform out-of-plane strain. In either case, if the deformation can be viewed as being consistent with the theory of plane stress in the region in which measurements are made, then the experimental information is related to the in-plane gradient of the first stress invariant, which has components $\partial(\sigma_{11}+\sigma_{22})/\partial x_\alpha$ for $\alpha = 1$ or 2.

If the terms in (18) are differentiated with respect to x_1 and then rearranged in order to isolate the term that would represent the stress intensity factor if the field were indeed a square root singular stress intensity factor field, it is found that

$$\frac{\sqrt{2\pi}r_l^{3/2}}{F(v)\cos\frac{3}{2}\theta_l}\frac{\partial(\sigma_{11}+\sigma_{22})}{\partial x_1} = K_I^d(t) + r_l\left[\beta_1(t)\frac{\cos\frac{1}{2}\theta_l}{\cos\frac{3}{2}\theta_l} + \beta_2(t)\frac{\cos\frac{5}{2}\theta_l}{\cos\frac{3}{2}\theta_l}\right]$$

$$+\beta_3(t)r_l^{3/2}\frac{1}{\cos\frac{3}{2}\theta_l} + r_l^2\left[\beta_4(t)\frac{\cos\frac{1}{2}\theta_l}{\cos\frac{1}{2}\theta_l} + \beta_5(t) + \beta_6(t)\frac{\cos\frac{7}{2}\theta_l}{\cos\frac{3}{2}\theta_l}\right]$$

$$+\beta_7(t)r_l^{5/2}\frac{\cos\theta_l}{\cos\frac{3}{2}\theta_l} + o(r_l^{5/2}), \quad (20)$$

where $F(v) = (1+\alpha_s^2)(\alpha_l^2-\alpha_s^2)/\Delta(v)$ and $\beta_1,\ldots,\beta_7$ are functions of time and crack tip velocity determined by the various coefficients in (18). As a matter of convenience, the left side of (20) will be denoted by $Y_I^d(r_l,\theta_l,t)$ in subsequent discussion. The important observation is that if, at any particular time, the near-tip stress field is accurately characterized by a square root singular stress intensity factor field over some region, then $Y_I^d(r_l,\theta_l,t)$ is independent of r_l and θ_l throughout that region. Furthermore, the value of Y_I^d at such a time is precisely the value of the corresponding dynamic stress intensity factor $K_I^d(t)$. On the other hand, if there is no region in the vicinity of the crack tip throughout which Y_I^d is uniform, then it must be concluded that the local crack tip field is not accurately represented by a stress intensity factor field. The quantity Y_I^d in (20) can be measured using the CGS method, and the question to be considered is whether or not the right side of this continued equality can describe the measured angular variation.

A selection of CGS interferograms obtained during dynamic crack propagation in impact-loaded, three-point-bend specimens of PMMA are shown in Fig. 2. These patterns were recorded by means of a rotating mirror high-speed camera and a pulsed laser light source; the details of the experimental setup are described by TIPPUR *et al.* (1991). In this case, the material is transparent and the method is used in transmission
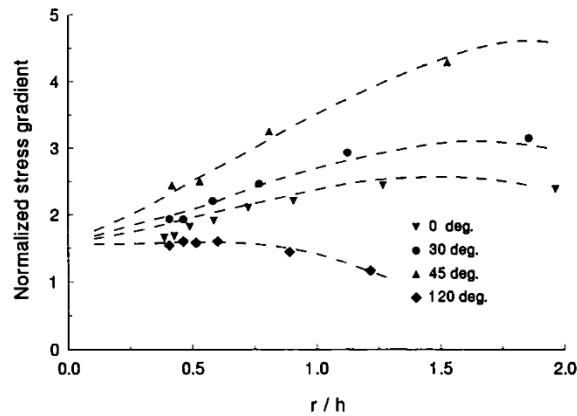
Fig. 3. Comparison of the radial variation of the experimental measurements of $Y_I^d(r_I, \theta_I, t)$ as defined by the left side of (20) with a fit to the expansion appearing as the right side of (20) for data obtained in transmission mode from one PMMA specimen (PD-11). The discrete points show the results of measurements, and the dashed curves are the result of a least-squares fit to the data.

mode. The fringes in Fig. 2 correspond to level curves of the quantity $\partial(\sigma_{11} + \sigma_{22})/\partial x_1$.

In the three-point-bend specimen of thickness h, the crack initiates abruptly from a blunted notch tip under the action of the stress wave loading provided by the impacting tup and, thereafter, it propagates at a nearly constant speed. Figure 3 shows the analysis of an interferogram at a time of $t = 20$ μs after crack growth initiation. The crack speed is approximately 300 m/s. In this early time after fracture initiation, it is expected that transient effects due to the abrupt initiation event and associated stress wave propagation are still important. Figure 3 shows the variation of Y_I^d vs normalized distance r_I/h as given in (20) along the radial lines corresponding to $\theta_I = 0$, 30, 45 or 120° emanating from the moving crack tip. It appears from Fig. 3 that there is no region (within the framework of plane stress) over which the measured Y_I^d is constant. Indeed, the observed values scatter by as much as several hundred percent about a mean value. Thus, there appears to be no region in which a square root singular stress intensity factor field dominates the near-tip field.

Figure 3 also includes the results of applying a least-squares procedure to fit the expression on the right side of (20) to the experimentally measured values of Y_I^d as obtained from the interferogram. The procedure is based on the values of Y_I^d measured at several points along each radial line. Because Y_I^d and r_I, θ_I are known at each such point, (20) provides a linear equation for values of β_k ($k = 1, \ldots, 7$) and K_I^d at each point. A best-fit solution of the overdetermined system of linear equations for β_k is then determined by a standard least-squares procedure. Each curve found in this way (shown as dotted in Fig. 3) corresponds to the transient expansion on the right side of (20) and each curve apparently captures the essential features of the data for all observations made outside of the zone of three-dimensional effects, namely, for $r_I > h/2$ (Rosakis and Ravi-Chandar, 1986). It is emphasized that the curves *all* correspond to the same values of β_k, so that the fit is consistent in both the radial and angular directions.
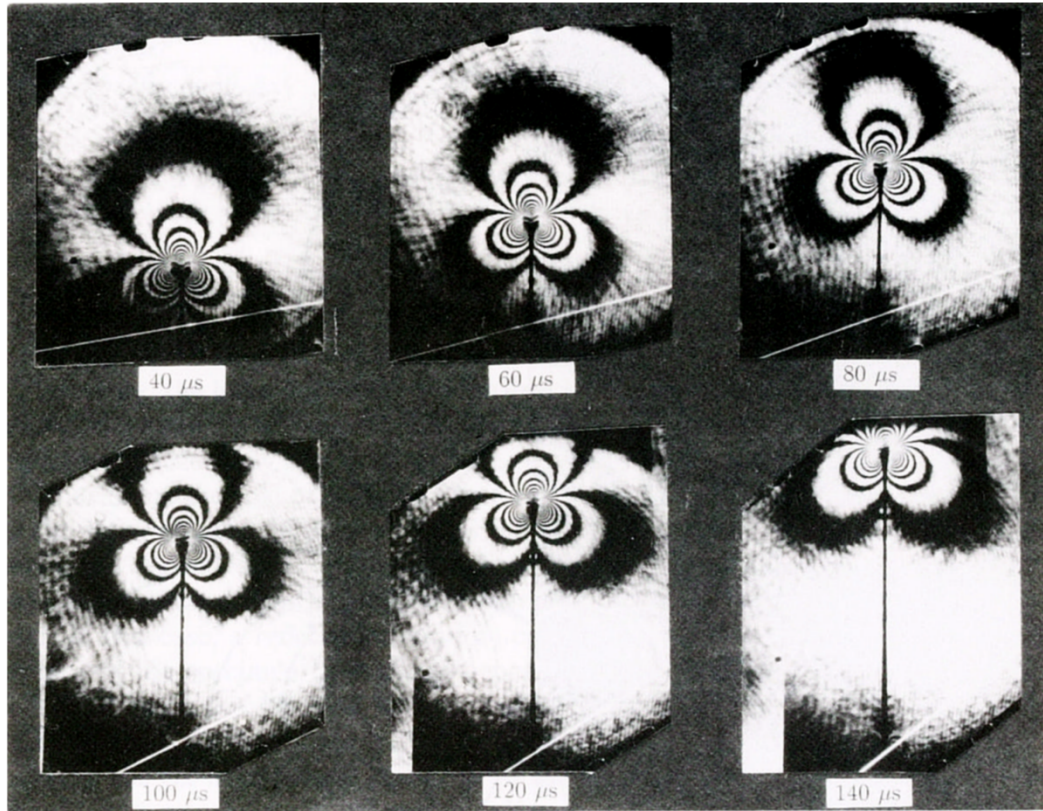
FIG. 2. Interferograms obtained during rapid crack propagation in impact-loaded, three-point-bend specimens of PMMA. The fringes are level curves of the gradient of the first stress invariant $\partial(\sigma_{11}+\sigma_{22})/\partial x_1$, and the times shown indicate the time elapsed since the onset of crack growth.
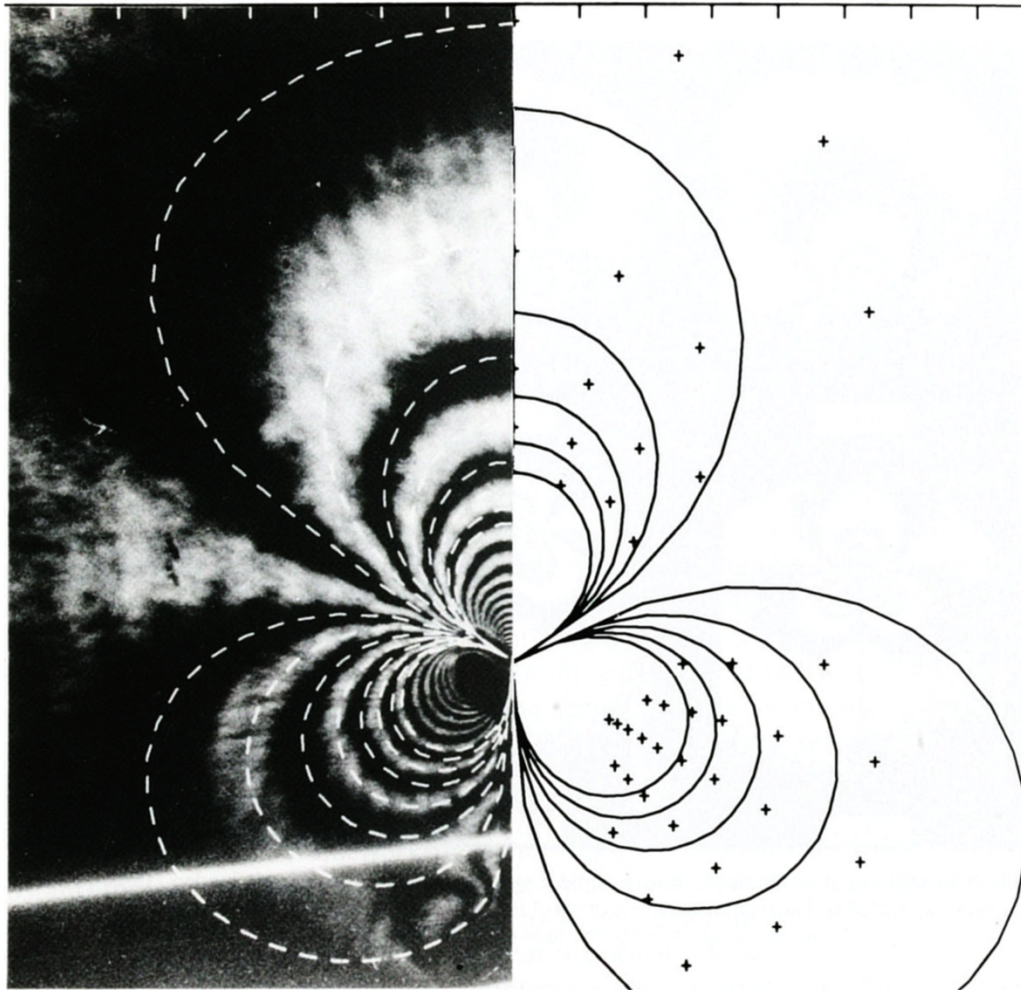
FIG. 4. Information on points of constant stress gradient in the x_1-direction obtained directly from the photograph on the left (specimen PD-11) is shown in the form of discrete points on the right side, and the fringe loops implied by the points match the actual loops on the left. For purposes of comparison, synthetic fringe patterns constructed from one-term (solid lines) and six-term (dashed lines) crack tip field expansions are also shown.

710

When the CGS method is applied in reflection mode, the fringes obtained correspond to level curves of $\partial u_3/\partial x_1$, where u_3 is the out-of-plane displacement of the surface of the specimen. For deformation corresponding to a state of plane stress,

$$\frac{\partial u_3}{\partial x_1} = -\frac{vh}{2E}\frac{\partial}{\partial x_1}(\sigma_{11}+\sigma_{22}).$$

In light of this relationship, the expression equivalent to (20) is

$$\frac{2\sqrt{2\pi}Er_l^{3/2}}{F(v)vh\cos\frac{3}{2}\theta_l\cos\frac{3}{2}\theta_l}\frac{\partial u_3}{\partial x_1} = K_l^d(t)+r_l\left[\delta_1(t)\frac{\cos\frac{1}{2}\theta_l}{\cos\frac{3}{2}\theta_l}+\delta_2(t)\frac{\cos\frac{5}{2}\theta_l}{\cos\frac{3}{2}\theta_l}\right]$$

$$+\delta_3(t)r_l^{3/2}\frac{1}{\cos\frac{3}{2}\theta_l}+r_l^2\left[\delta_4(t)\frac{\cos\frac{1}{2}\theta_l}{\cos\frac{3}{2}\theta_l}+\delta_5(t)+\delta_6(t)\frac{\cos\frac{7}{2}\theta_l}{\cos\frac{3}{2}\theta_l}\right]$$

$$+\delta_7(t)r_l^{5/2}\frac{\cos\theta_l}{\cos\frac{3}{2}\theta_l}+o(r_l^{5/2}), \quad (21)$$

where δ_k ($k = 1,\ldots,7$) are functions of crack tip speed and time. Again, for convenience, the left side of (21) is described by $Z_l^d(r_l,\theta_l,t)$. Just as in the case of Y_l^d above, the quantity Z_l^d is essentially constant in any region in which the fields are represented accurately by a square root singular stress intensity factor field.

To examine the role of higher-order terms in the near-field asymptotic expansion in the interpretation of data obtained by means of light *reflected* from the sample surface, a second series of dynamic fracture tests was conducted. In this series, the specimens were again impact-loaded three-point-bend specimens of PMMA. However, in this case, a reflective aluminum coating was deposited on the front planar surface of the specimen by vacuum deposition. The experimental arrangement for reflection mode described by KRISHNASWAMY *et al.* (1990) was used to observe the crack tip fields. In order to provide a full-field, visual demonstration of the agreement between the six-term fit and the experimental data, a reconstructed fringe pattern based on a least-squares fit of the data is shown in Fig. 4 (discrete points on the right side) superimposed on the actual interferogram (contrast fringes on the left side). In addition, the broken lines added to the left side of Fig. 4 represent the fringe pattern reconstructed from the full, higher-order least-squares fit. The higher-order fringe pattern clearly matches the observed fringes very well, except close to the crack tip where the large influence of three-dimensional effects precludes a direct comparison. For purposes of comparison, a synthetic fringe pattern generated from only the term in the crack tip field expansion associated with the stress intensity factor K_l^d is also shown as the solid lines in the right half of Fig. 4. This pattern differs significantly from the actual pattern, suggesting that the higher-order terms in (18) can have a significant influence on the crack tip stress field over the region in which fringes are commonly observed.

The discrete points in Fig. 5 show the variation of $Z_l^d(r_l,\theta_l,t)$ with radial distance r_l/h from the crack tip for several radial lines emanating from the crack tip. As in the corresponding case of transmission mode observations, the quantity Z_l^d is not constant over any significant part of the region of observation, as would be expected if the
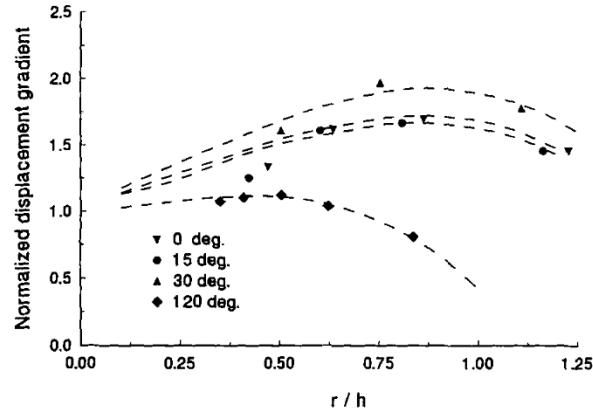
L. B. FREUND and A. J. ROSAKIS

FIG. 5. Comparison of the radial variation of the experimental measurements of $Z_I^d(r_l, \theta_l, t)$ as defined by the left side of (21) with a fit to the expansion appearing as the right side of (21) for data obtained in reflection mode from one PMMA specimen (PD-16). The discrete points show the results of measurements, and the dashed curves are the results of a least-squares fit to the data.
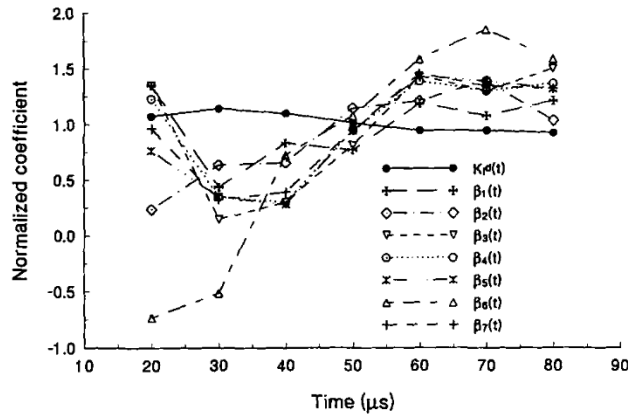

FIG. 6. Time histories of $K_I^d(t)$ and $\beta_k(t)$, each normalized by its mean value, for the duration of a particular crack propagation event.

deformation field there would be a square root singular stress intensity factor field. On the other hand, the discrete points representing measured values closely follow the curves obtained from a least-squares fit to the six-term asymptotic expansion, at least for $r_l/h > 0.5$.

To further illustrate the *transient* nature of the crack tip fields, the time histories of the stress intensity factor $K_I^d(t)$ and of the coefficients $\beta_k(t)$ inferred from the data during a representative dynamic fracture experiment are shown in Fig. 6. Each of the quantities is normalized by its mean value for the entire test. Even though the crack speed was constant during the entire observation, Fig. 6 clearly shows the transient nature of the crack growth process. For the first 50 μs after initiation of crack growth from a stationary blunted notch, there is significant fluctuation in the values of $\beta_k(t)$ ($k = 2, \ldots, 7$). The transient nature of a crack tip field of this kind during the

early stages of crack growth was anticipated in the analytical results of MA and FREUND (1986).

THE CASE OF TRANSIENT CRACK GROWTH AT NONUNIFORM VELOCITY

The foregoing analysis of near-tip fields during transient crack growth is restricted to the class of situations in which the crack speed is constant. As such, the analysis represents a full development of some ideas introduced in FREUND (1990). The case of transient crack growth at nonuniform speed can be treated in much the same way but, as might be expected, the details are more complicated. In this section, a three-term expansion for the first stress invariant is obtained.

As in the case of constant-speed crack growth, (7a) and (7b) have solutions

$$\hat{\Phi}_0(r_l, \theta_l, t) = A_0(t) r_l^{3/2} \cos \tfrac{3}{2}\theta_l,$$

$$\hat{\Phi}_1(r_l, \theta_l, t) = A_1(t) r_l^2 \cos 2\theta_l. \tag{22}$$

Up to this point, the expressions appear to be the same as for constant-speed growth. However, they differ in the fundamental respect that the coordinates r_l, θ_l are now functions of time. From their definitions, it is the crack speed that determines the degree of distortion of these coordinates from the physical polar coordinates, and the crack speed is now a function of time.

For $m = 2$, the governing equation (8) takes the form

$$\alpha_l^2 \frac{\partial^2 \Phi_2}{\partial \eta_1^2} + \frac{\partial \Phi_2}{\partial \eta_2^2} = -2\sqrt{v(t)} \frac{\partial}{\partial t} \left[\frac{\sqrt{v(t)}}{c_l^2} \frac{\partial \Phi_0}{\partial \eta_1} \right]. \tag{23}$$

If a transformation to polar coordinates (r_l, θ_l) is made and $(22)_1$ is used, (23) becomes

$$\nabla_l^2 \hat{\Phi}_2 = r_l^{1/2} \cos \tfrac{1}{2}\theta_l (D^{-1}[A_0] + 2B \sin^2 \tfrac{1}{2}\theta_l), \tag{24}$$

where

$$D^{-1}[A_0] = \frac{\sqrt{v(t)}}{\alpha_l^2 c_l^2} \frac{\mathrm{d}}{\mathrm{d}t} \left[\frac{4\sqrt{v(t)}(1+\alpha_s^2)}{\sqrt{2\pi}\mu\Delta(v)} K_I^d(t) \right]$$

$$B(t) = \frac{\sqrt{2\pi}v(t)^2(1+\alpha_s^2)}{c_l^4 \alpha_l^4 \mu \Delta(v)} K_I^d(t) \frac{\mathrm{d}v}{\mathrm{d}t}(t).$$

The general solution of (24) for mode I crack growth is

$$\hat{\Phi}_2(r_l, \theta_l, t) = r_l^{5/2} [\tfrac{1}{6} D^{-1}[A_0] \cos \tfrac{1}{2}\theta_l + B(\tfrac{11}{24}\cos \tfrac{1}{2}\theta_l - \tfrac{1}{2}\cos^3 \tfrac{1}{2}\theta_l) + A_2 \cos \tfrac{5}{2}\theta_l], \tag{25}$$

where it is clear that the last term is the homogeneous solution of the equation.

A three-term asymptotic expansion in powers of r_l for the first stress invariant can be obtained by substituting the expressions for $\hat{\Phi}_0(r_l, \theta_l, t)$, $\hat{\Phi}_1(r_l, \theta_l, t)$ and $\hat{\Phi}_2(r_l, \theta_l, t)$ into (10), with the result that

$$\frac{\sigma_{11}+\sigma_{22}}{2\rho(c_l^2-c_s^2)} = \frac{3v^2}{4c_l^2}A_0\frac{\cos\frac{1}{2}\theta_l}{r_l^{1/2}} + \frac{2v^2}{c_l^2}A_1$$

$$+\left\{\frac{15v^2}{4c_l^2}A_2\cos\frac{1}{2}\theta_l + D^{-1}[A_0]\left[\left(1-\frac{v^2}{2c_l^2}\right)\cos\frac{1}{2}\theta_l + \frac{v^2}{8c_l^2}\cos\frac{3}{2}\theta_l\right]\right.$$

$$+B\left[2\left(1-\frac{53v^2}{64c_l^2}\right)\cos\frac{1}{2}\theta_l - 2\left(1-\frac{3v^2}{2c_l^2}\right)\cos^3\frac{1}{2}\theta_l\right.$$

$$\left.\left.-\frac{7v^2}{2c_l^2}\cos^5\frac{1}{2}\theta_l + \frac{2v^2}{c_l^2}\cos^7\frac{1}{2}\theta_l\right]\right\}r_l^{1/2} + o(r_l^2). \tag{26}$$

It is readily verified that $B = 0$ for constant-speed crack growth, and that this expression reduces to the case of (18) of equivalent order. It is noted that crack tip acceleration enters the expansion only through the coefficients $D^{-1}[A_0]$ and B.

Explicit Expansion for the Broberg Solution

In order to illustrate the role of the higher-order terms in the near-tip expansion in a more explicit way, the solution of a particular boundary value problem concerned with elastodynamic crack growth is considered. This is the plane strain problem of a crack growing symmetrically from zero initial length at constant rate under uniform remote tensile stress σ_∞. The plane of deformation is the x_1', x_2'-plane and the crack lies in the interval $-vt < x_1' < vt$, $x_2' = 0$, where v is the constant speed of either crack tip. This is the problem first analyzed by Broberg (1960).

An expression for the first stress invariant directly ahead of the crack tips can be obtained from equations (6.3.43) and (6.3.50) of Freund (1990). On the plane $x_2' = 0$,

$$\sigma_{11}+\sigma_{22} = -2\sigma_\infty I(v/c_s)h\left(1-\frac{c_s^2}{c_l^2}\right)\int_{1/c_l}^{t/x}\frac{f(\xi)}{(h-\xi)^{3/2}}\,d\xi, \tag{27}$$

where $h = 1/v$, $I(v/c_s)$ is a known function of v, and $f(\xi) = (c_s^{-2}-2\xi^2)/(\xi^2-c_l^{-2})^{1/2}(h+\xi)^{3/2}$. Focusing on the crack tip moving in the positive x_1'-direction, if this expression is expanded in powers of $x_1 = x_1'-vt$ near $x_1 = 0$ then

$$\sigma_{11}+\sigma_{22} = W(v)\frac{K_I^d(t)}{\sqrt{2\pi}}\left\{\frac{1}{\sqrt{x_1}} + \frac{\sqrt{x_1}}{vt}\left[\frac{1}{2} + \frac{f'(h)h}{f(h)}\right]\right\} + o(\sqrt{x_1}), \tag{28}$$

where

$$W(v) = \frac{2(1+\alpha_s^2)(\alpha_l^2-\alpha_s^2)}{\Delta(v)},$$

$$K_I^d(t) = \frac{c_s^2 I(v/c_s)\Delta(v)}{v^2\alpha_l}\sigma_\infty\sqrt{\pi vt}.$$

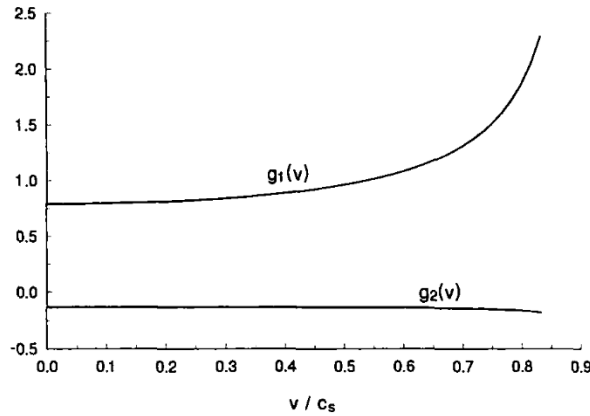If the expansion (28) is then compared with the general expansion (18) and terms

FIG. 7. Functions of crack tip speed appearing in (30) for $v = \frac{1}{3}$, as determined by the Broberg crack propagation solution.

of like powers in distance from the crack tip are equated, then explicit equations for the coefficients in the expansion are obtained as

$$A_1 = 0,$$

$$D^1[A_0]\left(1 - \frac{3v^2}{8c_l^2}\right) + A_2 \frac{15}{4} \frac{v^2}{c_l^2} = -\frac{W(v)K_I^d(t)}{2\mu(c_l^2/c_s^2 - 1)vt\sqrt{2\pi}}\left[\frac{1}{2} + \frac{f'(h)h}{f(h)}\right]. \qquad (29)$$

From its definition, $D^1[A_0]$ can be expressed in terms of the stress intensity factor. Consequently, the coefficients of the two terms in (18) corresponding to the particular and homogeneous solutions of the differential equation for $m = 3$ in the asymptotic expansion (18) are

$$D^1[A_0] = g_1(v)\frac{K_I(t)}{\mu vt\sqrt{2\pi}},$$

$$A_2\frac{v^2}{c_l^2} = g_2(v)\frac{K_I(t)}{\mu vt\sqrt{2\pi}}, \qquad (30)$$

where the two functions of crack tip speed $g_1(v)$ and $g_2(v)$ are shown in Fig. 7 for Poisson's ratio $v = 1/3$.

In view of the fact that the coefficients in (30) are proportional to $t^{1/2}$, it is evident that the third term in the near-tip asymptotic expansion of the first stress invariant can be very large during the early stages of crack growth, possibly dominating the square root singular term under certain conditions. This result clearly illustrates the strong bearing that transients may have on the question of K_I^d-dominance of the near-tip field, even if the crack tip speed is constant.

CONCLUDING REMARKS

Motivated by the wave propagation characteristics of the fields in the vicinity of a growing crack tip, an approximation of the near-tip field in the form of an asymptotic

expansion has been introduced. The leading term in the expansion of the local stress field is the familiar stress intensity factor contribution, that is, it is square root singular in the radial distance from the crack tip and its coefficient is proportional to the instantaneous value of the stress intensity factor. The higher-order terms, on the other hand, take into account the recent past history of the stress intensity factor and crack motion, in order to reflect the transient nature of the local field. These terms involve the time derivatives of the stress intensity factor $K_I^d(t)$ and crack speed $v(t)$. The expansion is based on an assumption that the fields are indeed two-dimensional right up to the crack tip.

For the case of constant crack speed but time-dependent stress intensity factor, the expansion is given explicitly to six terms. The coefficients are evaluated on the basis of experiments involving dynamic crack growth in PMMA plates under the assumed conditions. The measurements of the crack tip field were obtained by means of the full-field CGS method. The experimental results, in the form of a gradient of the first invariant of stress in the direction of crack growth, appear to be well described by the expansion. More precisely, over the region near the crack tip where the elastodynamic field is expected to be essentially a two-dimensional plane stress field, both the observed radial and angular variation of the data are consistent with the higher-order expansion.

The good agreement between observation and the higher-order expansion also has a disconcerting aspect. As noted above, the experimental results and the expansion are in close agreement over a region of significant size around the crack tip. However, during the earlier phase of crack propagation, nowhere within this region of agreement is the field dominated by a stress intensity factor field. In other words, even though the specimen is large enough so that reflected waves do not influence the local fields, the transient nature of the stress field during the early phase of crack growth prevents a complete stress intensity factor from becomining established outside the near-tip three-dimensional zone. This feature erodes the value of the stress intensity factor concept in characterizing the fracture resistance of the material. From the discussion of the observations in connection with Figs 3 and 5, it is clear that a unique plane stress intensity factor can be identified in both the data and the model at each instant of time. Furthermore, Fig. 6 shows that the inferred value of the stress intensity factor is nearly constant during growth, even though no fully developed stress intensity factor field is apparent. However, this stress intensity factor is not strictly relevant in the spirit of fracture toughness testing. The dilemma is particularly acute for the case of plane stress where a region very close to the crack edge is dominated by three-dimensional effects, and therefore measurements in this region cannot be used in any two-dimensional analysis of fields. The restriction is much less severe for the case of plane strain crack growth.

A re-examination of the experimental results of RAVI-CHANDAR and KNAUSS (1987) suggests that this may be an illustration of the transient phenomena discussed in this paper. In this investigation the optical method of caustics in transmission mode was used to measure the stress intensity factor history of a crack which is loaded dynamically by the direct application of a pressure pulse on its faces. In each case, uniform crack face pressure was imposed. Its magnitude σ_0 increased linearly in time from a nominally zero initial value to a predetermined final value, with the duration of the increase always being about $T = 25$ μs. After initiation, the crack propagated with

nearly constant speed v. A series of experiments corresponding to different final crack face pressure values, and therefore different rates of loading up to fracture initiation, were reported. Figure 8 shows a comparison of stress intensity factor time histories obtained analytically and measured experimentally by caustics. The lower curve in Fig. 8 demonstrates good agreement between experiment and theory during both the dynamic loading stage of the stationary crack and crack growth. On the other hand, the upper curve in Fig. 8, which corresponds to a higher rate of loading, shows excellent agreement of theory and measurements only up to the point of crack initiation. After the crack started propagating, the experimentally obtained stress intensity factor K_I^d overestimates the theoretical result by almost 50%. It should be noted that the delay time τ for the crack to initiate after the application of the loading pulse is a factor of 3 greater in the experiment corresponding to the lower curve in Fig. 8 than in the experiment corresponding to the upper curve. The resulting crack tip speed in the former figure is also about half that in the latter. It is thus expected that transient higher-order effects of the type demonstrated above become more pronounced in the case of the upper curve. If it is recalled that the analysis of the optical caustics patterns is based on the assumption that the near crack tip field is represented solely by the $r^{-1/2}$ singular term of the asymptotic expansion (K_I^d-dominance) then the suspicion arises that caustics may not be measuring the correct values of K_I^d after crack initiation. This becomes more pronounced in the higher-rate experiments, where higher-order transient effects result in a violation of the basic assumption upon which the analysis of optical caustics is made.

An alternative illustration of the same phenomenon is seen in the results of KRISHNASWAMY and ROSAKIS (1990). In this work a "bifocal" caustics arrangement is used to investigate dynamic crack initiation and growth in AISI 4340 steel. At each time during dynamic crack growth the high-speed camera used in the experiment
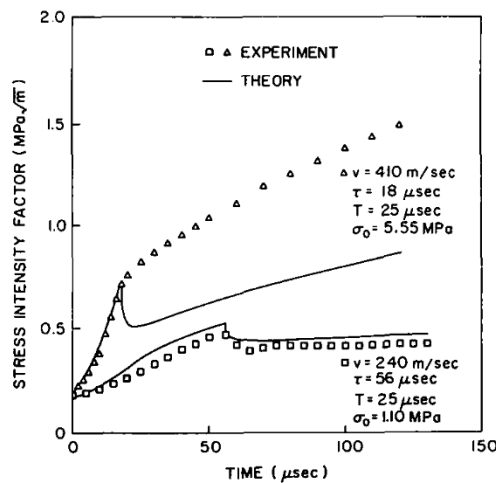

FIG. 8. Dynamic stress intensity factor vs time for fracture initiation and propagation in Homalite-100 due to sudden application of crack face pressure (RAVI-CHANDAR and KNAUSS, 1987). With reference to the legends, σ_0 is the level of crack face pressure achieved after rise time T, and the crack begins to propagate at constant speed v after elapsed time τ from the instant that loading begins.

simultaneously records two caustic patterns formed from two initial curves at different distances from the crack tip. Both caustics are then interpreted on the basis of the conventional analysis with K_I^d-dominance. Since both caustics are formed from points surrounding the tip which lie outside of the near-tip three-dimensional zone, the values of the stress intensity factor obtained by bifocal caustics pairs are expected to be identical unless the assumption of K_I^d-dominance is violated. The experimental results show differences in K_I^d values of up to 40%. This suggests that higher-order transient terms of the nature discussed in this paper should be included in the analysis of optical caustics in order for the method to furnish accurate values of stress intensity factors.

A long-standing issue of fundamental importance in dynamic fracture research is the connection between the dynamic fracture toughness and the crack tip velocity. The debate, for the most part, has centered around the question of uniqueness of a relationship between K_I^d and v. KOBAYASHI and DALLY (1980), ROSAKIS et al. (1984) and ZEHNDER and ROSAKIS (1989), among others, provided data sets that seem to indicate that the K_I^d–v relation is reasonably viewed as a material property. On the other hand, the results of KOBAYASHI and MALL (1978) and RAVI-CHANDAR and KNAUSS (1984), based on photo-elasticity and the method of caustics in transmission, respectively, suggest that there is no such correspondence. While this difference may be attributable to differences in material characteristics or experimental conditions, the fundamenal difficulty of achieving a well-developed stress intensity factor field in transient crack growth experiments may also be playing a significant role.

Another series of experiments leading to results that have yet to be explained are those reported by KALTHOFF (1983), which seem to indicate that the dynamic fracture toughness could be specimen-dependent. In this case, as well, it may be possible to attribute the apparent specimen dependence of K_I^d to specimen-dependent differences in the near-tip region. Remarks on such observations are, of course, speculative at this point, and further study is required to assess the possibilities.

On the basis of some crack propagation experiments in which the optical method of caustics was used, TAKAHASHI and ARAKAWA (1987) proposed that the instantaneous value of the dynamic fracture toughness of their material depended on the instantaneous crack tip acceleration. As shown in this investigation, however, the near-tip stress field expansion involves crack tip acceleration in its third- or higher-order terms [see (26), for example]. As a result, caustic patterns obtained from regions where higher-order terms are important will exhibit acceleration effects. However, if caustics from such a region are *interpreted* on the assumption of K_I^d-dominance then it would appear that the instantaneous value of the stress intensity factor, and thus of the fracture toughness of the material, depends on the instantaneous acceleration of the crack tip.

The re-examination of the crack tip stress field for elastodynamic crack growth under transient conditions has led to certain features of the near-tip field that have the potential for significantly altering the crack tip field from the commonly assumed square root singular stress intensity factor field. Furthermore, a particular data set has been examined in light of the theoretical findings, with the result that the data are well described by a higher-order representation of the transient crack tip field. These results offer hope of resolving some long-standing paradoxes in the area of dynamic fracture, and speculation along these lines has been offered in this section. In pursuing

this issue, full-field optical techniques such as CGS or photoelasticity naturally are advantageous because interpretation of data and thus measurement of K_I^d does not hinge on the assumption of K_I^d-dominance. For both techniques a higher-order transient analysis of the type presented above can be used to obtain the relevant coefficients as a function of time. On the other hand, it may be possible to refine the analysis of caustics with the hope that the technique may exhibit the necessary sensitivity to provide information of the kind needed to assess the importance of higher-order terms in the crack tip field expansion. Given the extraordinary experimental simplicity of the technique this seems to be a worthwhile task for future research.

REFERENCES

BROBERG, K. B. 1960 *Arch. Fisik* **18**, 159.

DALLY, J. W. 1987 In *Static and Dynamic Photoelasticity and Caustics* (edited by A. LAGARDE), p. 247. Springer, New York.

FREUND, L. B. 1990 *Dynamic Fracture Mechanics*. Cambridge University Press, Cambridge.

IRWIN, G. R. 1957 *J. appl. Mech.* **24**, 361.

KALTHOFF, J. F. 1983 In *Workshop on Dynamic Fracture* (edited by W. G. KNAUSS, K. RAVI-CHANDAR and A. J. ROSAKIS), p. 11. California Institute of Technology, Pasadena, CA.

KOBAYASHI, A. S. and MALL, S. 1978 *Expl Mech.* **18**, 11.

KOBAYASHI, T. and DALLY, J. W. 1980 In *Crack Arrest Methodology* (edited by G. T. HAHN and M. F. KANNINEN), ASTM STP 711, p. 89. ASTM, Philadelphia, PA.

KRISHNASWAMY, S. and ROSAKIS, A. J. 1991 *J. appl. Mech.* **58**, 87.

MA, C. C. and FREUND, L. B. 1986 *J. appl. Mech.* **53**, 303.

RAVI-CHANDAR, K. and KNAUSS, W. G. 1984 *Int. J. Fracture* **25**, 247.

RAVI-CHANDAR, K. and KNAUSS, W. G. 1987 *J. appl. Mech.* **54**, 72.

ROSAKIS, A. J., DUFFY, J. and FREUND, L. B. 1984 *J. Mech. Phys. Solids* **32**, 443.

ROSAKIS, A. J. and RAVI-CHANDAR, K. 1986 *Int. J. Solids Struct.* **22**, 121.

TAKAHASHI, K. and ARAKAWA, K. 1987 *Expl Mech.* **27**, 195.

TIPPUR, H. V., KRISHNASWAMY, S. and ROSAKIS, A. J. 1991 *Int. J. Fracture* (to appear).

YANG, W. and FREUND, L. B. 1985 *Int. J. Solids Struct.* **21**, 977.

ZEHNDER, A. T. and ROSAKIS, A. J. 1990 *Int. J. Fracture* **43**, 271.